

Journal of Biomedical Optics

BiomedicalOptics.SPIEDigitalLibrary.org

Spatially extended versus frontal cerebral near-infrared spectroscopy during cardiac surgery: a case series identifying potential advantages

Christian Rummel
Reto Basciani
Arto Nirikko
Gerhard Schroth
Monika Stucki
David Reineke
Balthasar Eberle
Heiko A. Kaiser

SPIE.

Christian Rummel, Reto Basciani, Arto Nirikko, Gerhard Schroth, Monika Stucki, David Reineke, Balthasar Eberle, Heiko A. Kaiser, "Spatially extended versus frontal cerebral near-infrared spectroscopy during cardiac surgery: a case series identifying potential advantages," *J. Biomed. Opt.* **23**(1), 016012 (2018), doi: 10.1117/1.JBO.23.1.016012.

Spatially extended versus frontal cerebral near-infrared spectroscopy during cardiac surgery: a case series identifying potential advantages

Christian Rummel,^a Reto Basciani,^b Arto Nirikko,^c Gerhard Schroth,^a Monika Stucki,^b David Reineke,^d Balthasar Eberle,^b and Heiko A. Kaiser^{b,*}

^aUniversity of Bern, Support Center for Advanced Neuroimaging, University Institute for Diagnostic and Interventional Neuroradiology, Inselspital, Bern, Switzerland

^bUniversity of Bern, Department of Anesthesiology and Pain Therapy, Inselspital, Bern, Switzerland

^cUniversity of Bern, Department of Neurology, Schlaf-Wach-Epilepsie-Zentrum, Inselspital, Bern, Switzerland

^dUniversity of Bern, Department of Cardiovascular Surgery, Inselspital, Bern, Switzerland

Abstract. Stroke due to hypoperfusion or emboli is a devastating adverse event of cardiac surgery, but early detection and treatment could protect patients from an unfavorable postoperative course. Hypoperfusion and emboli can be detected with transcranial Doppler of the middle cerebral artery (MCA). The measured blood flow velocity correlates with cerebral oxygenation determined clinically by near-infrared spectroscopy (NIRS) of the frontal cortex. We tested the potential advantage of a spatially extended NIRS in detecting critical events in three cardiac surgery patients with a whole-head fiber holder of the FOIRE-3000 continuous-wave NIRS system. Principle components analysis was performed to differentiate between global and localized hypoperfusion or ischemic territories of the middle and anterior cerebral arteries. In one patient, we detected a critical hypoperfusion of the right MCA, which was not apparent in the frontal channels but was accompanied by intra- and postoperative neurological correlates of ischemia. We conclude that spatially extended NIRS of temporal and parietal vascular territories could improve the detection of critically low cerebral perfusion. Even in severe hemispheric stroke, NIRS of the frontal lobe may remain normal because the anterior cerebral artery can be supplied by the contralateral side directly or via the anterior communicating artery. © 2018 Society of Photo-Optical Instrumentation Engineers (SPIE) [DOI: 10.1117/1.JBO.23.1.016012]

Keywords: neuroimaging; spectroscopy; near-infrared; cardiovascular surgical procedures; patient outcome assessment; infarction; middle cerebral artery.

Paper 170177RR received Mar. 20, 2017; accepted for publication Dec. 19, 2017; published online Jan. 22, 2018.

1 Introduction

Stroke is one of the most serious complications of cardiac surgery. The reported incidence varies from <1% to 17% depending on the procedure, whether the studies have been performed prospectively or retrospectively, and patient comorbidities and time frame of follow-up.^{1–3} Depending on the procedure, between 57% and 84% of strokes are diagnosed during the first two postoperative days, with one-third estimated to occur during anesthesia and surgery.^{2,4} Perioperative stroke is associated with increased mortality, increased time on the ICU, and the possibility of long-term neurological deficits.^{2,4} The underlying pathophysiology of those neurological events is postulated to be either embolic (from atrial fibrillation or atherosclerotic plaque), thrombotic, or due to hypoperfusion intra- or postoperatively and may be aggravated by an inflammatory response.^{5,6}

Cerebral near-infrared spectroscopy (NIRS) is a promising technique to reduce the number and consequences of stroke during cardiac surgery by monitoring regional cerebral oxygen saturation.^{7–9} NIRS-derived cortical oxygenation was found to

correlate significantly with transcranial Doppler measures of middle cerebral artery (MCA) blood velocity and, hence, perfusion.¹⁰ As NIRS-based oximetry does not differentiate between arterial or venous blood, it rather represents a measure of equilibrium of oxygen delivery and consumption.¹¹

Numerous observational studies suggest that the duration and depth of desaturation events observed by NIRS could be associated with worse neurological outcome, but convincing evidence is still missing to date.⁷ A recent multicenter investigation tested the concept of an intervention algorithm for reversing desaturation events and reported an incidence—defined as >20% decline from preanesthesia baseline—of 61% during cardiopulmonary bypass (CPB).¹² The most effective intervention was correcting hypotension, which was successful in 30% of desaturation events on CPB. This underlines the importance of keeping the mean arterial pressure (MAP) on CPB above the lower limit of cerebral autoregulation to adequately perfuse the brain.^{13,14}

Commercially available two-channel NIRS monitoring is spatially restricted to the frontal brain and thus only reflects oxygenation changes in a part of the perfusion territory of

*Address all correspondence to: Heiko A. Kaiser, E-mail: heiko.kaiser@insel.ch

the anterior cerebral artery (ACA). Accordingly, frontally placed NIRS can only detect malperfusion of an entire hemisphere or of brain regions supplied by the right or left ACA. It is known, however, that only about 1.4% to 3% of cerebral emboli end up occluding the ACA, whereas the vast majority of occlusions occur within branches of the MCA.^{15,16} Moreover, in 8% to 13% of patients both ACAs are supplied by only one internal carotid artery (ICA) due to an absent or hypoplastic A1 segment of the circle of Willis (CoW).^{17–19} When monitoring is restricted to assessing frontal lobe perfusion, even widespread cerebral perfusion changes due to problems with the other carotid artery can remain undetected.¹⁶ In a previous study, we have already shown that using multichannel continuous-wave near-infrared spectroscopy (CW-NIRS) to evaluate the effectiveness of collateral circulation might serve as an objective and early predictive marker of critical perfusion during percutaneous transluminal angioplasty or balloon occlusion testing of an ICA.²⁰ CW-NIRS has a unique spatial and temporal resolution to explore local regulation of cerebral blood flow and metabolism.²¹

Thus, we tested the potential advantage of a spatially extended CW-NIRS system in detecting critical desaturation events in comparison with spatially restricted frontal NIRS in three cardiac surgical patients.

2 Methods

2.1 Patients

For this observational study, we enrolled three adult patients undergoing cardiac surgery on CPB. The pilot study was approved by the ethics committee of the Canton of Bern. All patients gave their written informed consent for participation. Anesthesia and surgical management were performed according to institutional standard operating procedures and clinical judgment of the responsible attending physician. The STROBE checklist for observational studies was used to guide the methods of this project and to structure this article.²²

2.2 Data Acquisition

We used the multichannel CW-NIRS system FOIRE-3000 (Shimadzu, Japan) with 16 transmitters/sources and 16 receivers/detectors. It measures light attenuation $A = \log(I_0/I)$ as a function of input (I_0) and output intensities (I) at three wavelengths (780, 805, and 830 nm) in the near-infrared spectrum. Light sources were selectively switched on consecutively for 16 ms (about 10^{13} wave cycles) and attenuation was measured at all detectors. For our purposes, we chose a setting where sources with spatial separation of at least 9 cm were allowed to be switched on at the same time. This led to a sampling rate of 10 Hz.

For data acquisition in the operating room (OR), a whole-head fiber holder of the FOIRE-3000 was mounted during patient preparation for cardiac surgery. We used an optode montage with 21 channels at 30-mm source–detector (SD) separation and 38 channels at 42-mm SD separation,²⁰ which was suitable for patients in supine position and allowed us to monitor parts of the vascular territories of the MCA and ACA of both hemispheres. Figure 1(a) shows approximate transmitter and receiver positions, together with the sampling regions of a selection of NIRS channels (yellow numbers) projected onto the pial surface of a healthy subject.

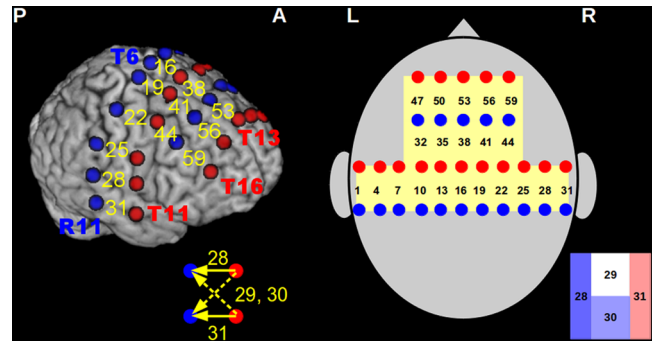


Fig. 1 Optode positions of spatially extended NIRS. (a) NIRS transmitter (red) and receiver (blue) positions. Approximate positions of brain regions monitored by NIRS signals recorded over 30-mm SD separation are indicated by yellow channel numbers. Below we show the schematics for channels 28 to 31 of NIRS channels measured over 30-mm (solid lines) and 42-mm SD distance (dashed lines). The two 42-mm channels 29 and 30 measure the hemoglobin concentration changes at the same location independently. 42-mm channels are assumed to have larger brain contribution than 30-mm channels. (b) Schematics showing that extended parts of the perfusion territories of the left and right MCA and ACA are monitored by this configuration. For clarity, we indicate the numbers of 30 mm channels only. In the color maps of Figs. 4, 6, 8, and 9, all 30-mm channels are symbolized by vertical strips centered between the transmitter and receiver optode. 42-mm channels measuring at the same location are represented by piled squares in between. To avoid visual bias, the area has identical size for all channels. P, posterior; A, anterior; L, left; and R, right.

According to the autocalibration function of the FOIRE-3000, all 59 NIRS channels had sufficient intensities in all patients. During measurements, time markers were set manually in the FOIRE-3000 to indicate clinically important time points, which were phases of potential hemodynamic instability and/or changes in cerebral perfusion, i.e., a MAP reduction of >20% of baseline, MAP support with norepinephrine, sternotomy, arterial, and venous cannulation, aortic cross clamping, commencement and termination of CPB, hypothermic circulatory arrest (HCA), selective antegrade cerebral perfusion (SACP), decrease or increase in pump flow, and reinstatement of pulsatile flow. To backtrace potential movement artifacts that usually manifest themselves as rapid and high amplitude changes in NIRS signals, markers were also set when the operation table or the patient's body was moved.

2.3 Data Processing

Using the modified Beer–Lambert law,²³ light attenuation time series $A(t)$ were channel-wise converted into relative concentration changes of oxyhemoglobin $\Delta[\text{oxyHb}]$ and deoxyhemoglobin $\Delta[\text{deoxyHb}]$. In principle, only two wavelengths are required to solve the linear system of equations. The redundant measurement at a third wavelength, however, can be used to reduce errors in presence of artifacts.

Changes of total hemoglobin $\Delta[\text{totalHb}] = \Delta[\text{oxyHb}] + \Delta[\text{deoxyHb}]$ and of the difference $\Delta[\text{diffHb}] = \Delta[\text{oxyHb}] - \Delta[\text{deoxyHb}]$ were also calculated. $\Delta[\text{totalHb}]$ is proportional to changes of the cerebral blood volume, whereas $\Delta[\text{diffHb}]$ is a marker for blood oxygenation changes. Although $\Delta[\text{diffHb}]$ does not provide absolute saturation values, it gives information similar to the tissue oxygenation index or total oxygen saturation (StO₂) of commercially available frontal NIRS monitors.²⁴

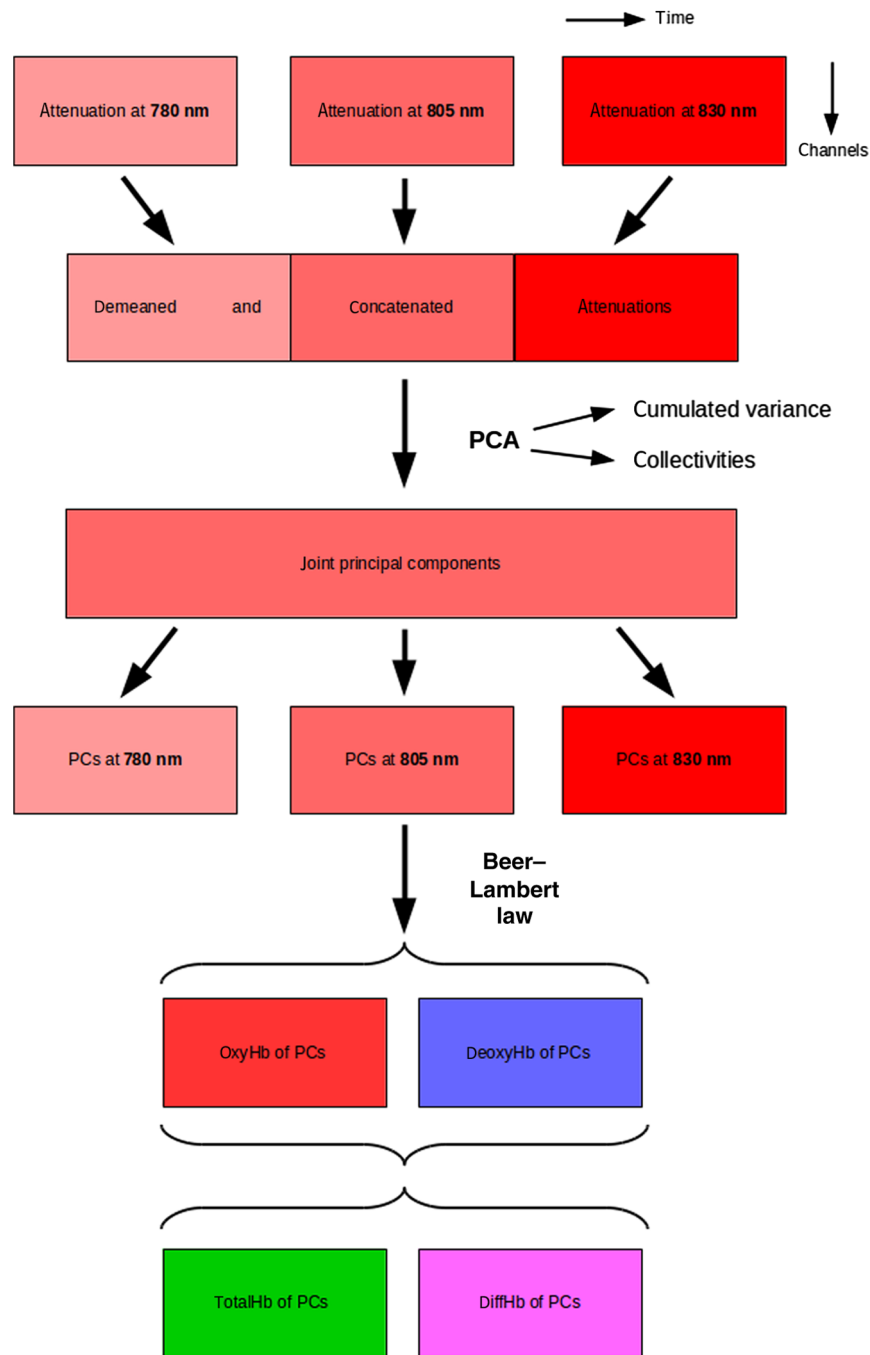


Fig. 2 Schematics of the PCs analysis strategy. Data matrices are symbolized by rectangles.

Table 1 Demographic data and surgical details.

Patient	Age	Gender	BMI	Procedure	CPB time	HCA time	SACP time	CPB priming
#1	69	male	25.7	AVR and two vessel CABG	94	—	—	1500
#2	77	male	23.1	Three vessel CABG	72	—	—	600
#3	76	male	21.8	Ascending aorta and hemiarch replacement	114	14	10	1500

Note: Age is depicted in years, times in minutes, and priming in milliliters. BMI, body mass index; CPB, cardiopulmonary bypass; HCA, hypothermic cardiac arrest; SACP, selective antegrade cerebral perfusion; AVR, aortic valve replacement; and CABG, coronary artery bypass graft.

In addition to channel-wise analysis, attenuation time courses of all 59 channels were decomposed using principal components analysis (PCA).²⁵ PCA is a technique to simplify a multivariate set of possibly correlated observables \vec{A} by linear transformation from the original signals to uncorrelated “principal components” (PC) \vec{P} by $\vec{P} = O\vec{A}$.

The required orthogonal transformation O can be found uniquely by diagonalization of the data’s covariance matrix, and the PCs can be ordered uniquely by decreasing fraction of total variance. In our case of spatially distributed sampling of a physiological time series $A_i(t)$, $i = 1, \dots, 59$, one obtains transformed time series $P_i(t)$, which represent certain “common features” of the recordings, along with spatial maps O_i indicating how much and with which algebraic sign these features are represented at a certain position.

Separate PCA decomposition of light attenuations at the three wavelengths would make later calculation of chromophore concentration changes from the PCs impossible. For this reason, we treated all wavelengths (and derived chromophore concentration changes) on the same footing. Attenuations at the three wavelengths were first demeaned channel-wise and concatenated in time (Fig. 2) and then the joint PCs were calculated. This procedure is more sensitive to coordinated variability in the data than separate PCA. The joint PCs were split up into their wavelength-specific parts for calculation of

PC-specific hemoglobin concentration changes. As only relative concentration changes can be calculated from the modified Beer–Lambert law,²³ restoration of the mean attenuations was not necessary.

2.4 Data Analysis

Movement artifacts were infrequent in all three surgical procedures. However, movements according to the marker lists were considered as potential confounders when interpreting the results.

The time course of attenuation and hemoglobin concentration as well as the spatial maps were visually inspected for all PCs. PC time courses that showed their main volatility near artifact markers or had dominant high-frequency components that could not be of physiological origin were excluded from further analysis. We also excluded PCs with nonsmooth spatial maps, where adjacent channels frequently showed weights with different algebraic signs. The NIRS recordings of a first test patient were corrupted by major artifact and thus had to be excluded entirely from further analysis.

To determine whether a PC contributed to many of the $M = 59$ signals with similar strength or just to a few, the collectivity of the corresponding spatial map O_i was calculated^{26,27}

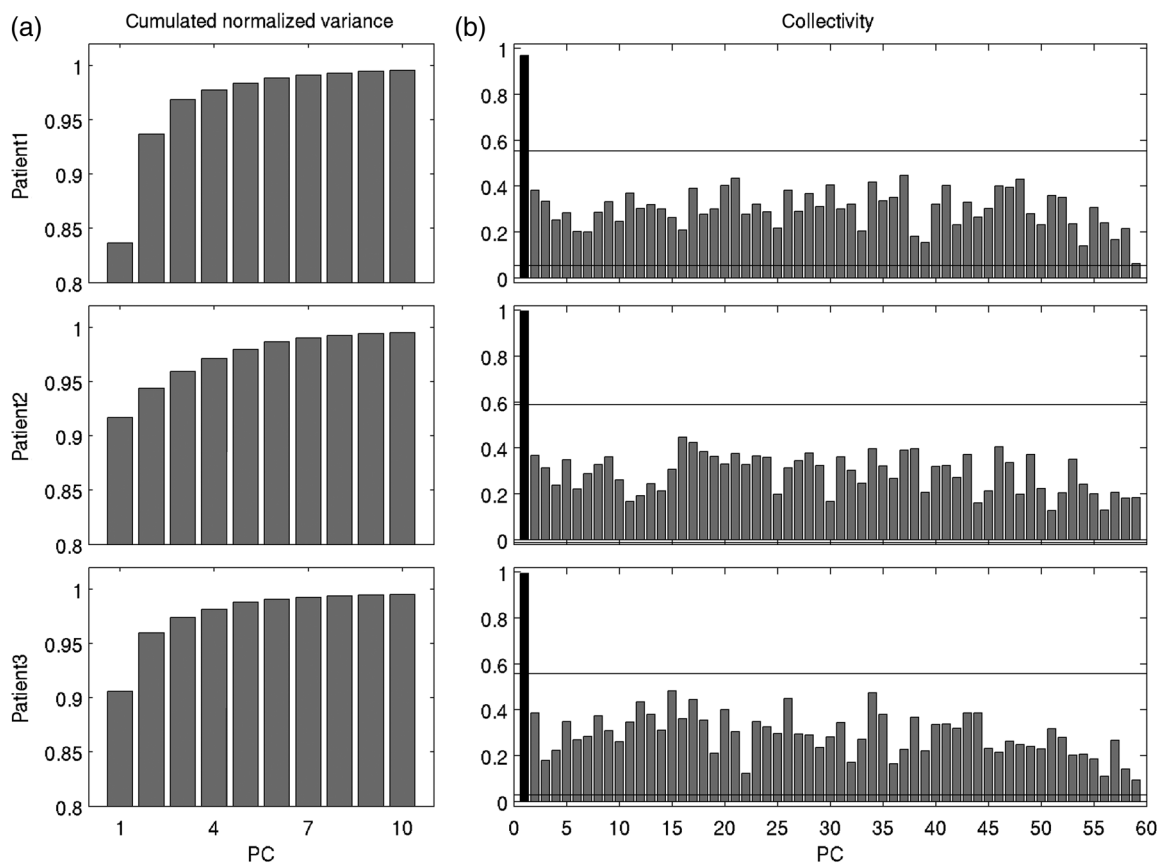


Fig. 3 Properties of the PCA decomposition matrices. (a) The cumulated normalized variances are shown for PCs 1 to 10 only. For higher PCs, these values are very close to one. (b) Collectivities of the eigenvectors. Global components are displayed as black bars. When falling into the interval $[0,1]$, the thresholds for detection of global and local components are shown as horizontal lines.

$$\text{coll}_i = \frac{1}{M \sum_{j=1}^M O_{ji}^4},$$

where the summation index j runs over the elements of the map vector O_i . Collectivity equals 1 if a PC contributes to all signals equally and $1/M$ if it contributes only to one out of M signals. We coined PCs as “global” if they had extraordinarily large collectivity [larger than the third quartile plus 1.5 times the interquartile range (IQR) of all PCs] and as “local” if they had extraordinarily small collectivity (smaller than the first quartile minus $1.5 \times \text{IQR}$).

For comparison of our multichannel NIRS measurement with the established bifrontal measurements, we assessed the mean contribution of each PC to the signals measured at the right (channels 56 to 59, see Fig. 1) and left forehead (channels 47 to 50). To identify events that were missed by frontal NIRS, we used a one-sided t -test to check for each PC whether it contributed less than expected by the average $1/M$ to these channels [significance level $\alpha = 0.05$, false-discovery-rate correction (FDR) for multiple comparisons].²⁸

3 Results

Demographic data and surgical details are shown in Table 1. With the exception of patient #3, the patients had an uneventful postoperative course.

PCs are numbered from largest variance (PC1) to smallest variance (PC59) and their main properties are summarized in Fig. 3. In all three patients, the first three PCs represented $>95\%$ of the cumulated normalized variance. According to our quantitative collectivity criteria, PC1 was categorized as the only “global” component in all three patients. The high values of collectivity and fraction of normalized variance of this component become evident as shown in Fig. 3.

In Fig. 4, we show the evolution of relative hemoglobin concentration changes associated with PC1 normalized to zero mean and unit variance over the whole surgical procedure. In Figs. 8 and 9 of the Appendix, the same is shown for PC2 and PC3. The start of CPB was associated with sudden variations in PC1 in all patients. The corresponding spatial maps on the right of Fig. 4 demonstrate that PC1 was represented almost equally strong and with equal sign in all 59 NIRS channels, including the frontal ones.

We focus on the time series of totalHb and diffHb for PC1 to PC4 during start of CPB as shown in Fig. 5. Importantly, the OR table was not moved and no movement artifacts were present in any of the patients in this phase of the recordings. In all patients, PC1 revealed a uniform concentration drop of totalHb and diffHb, which followed the hemodilution caused by the inflow of the asanguineous CPB prime. This expected signal shape was clearly visible also in the frontal channels on the left (channels 47 to 50) and the right (channels 56 to 59) in all patients (data

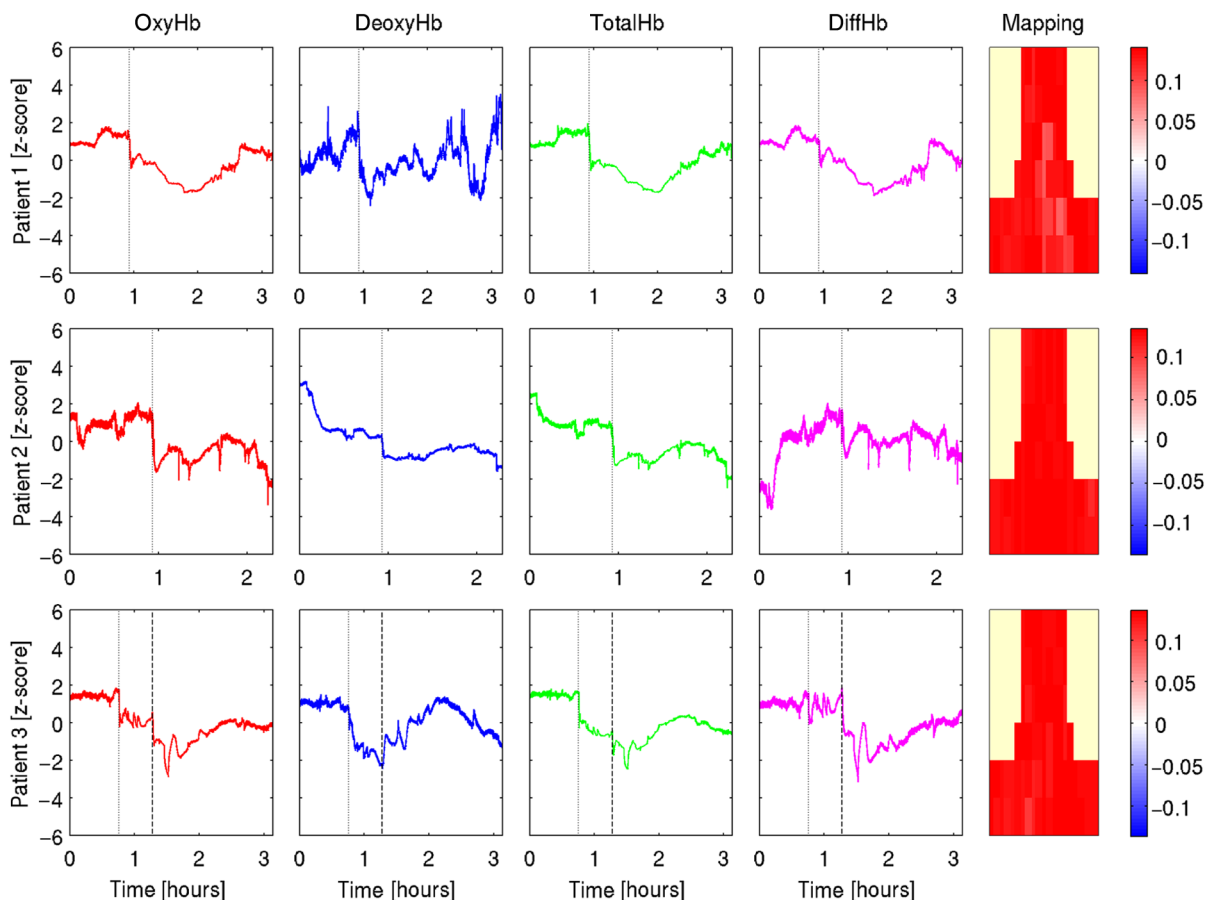


Fig. 4 Temporal evolution and spatial maps of the first PC1. Displayed are the full intraoperative recordings. CPB start is indicated by dotted vertical lines and HCA start in patient 3 by dashed vertical lines. For spatial orientation of the maps and interpretation of the patches, refer to the right part of Fig. 1. No signals were recorded in the yellow shaded areas.

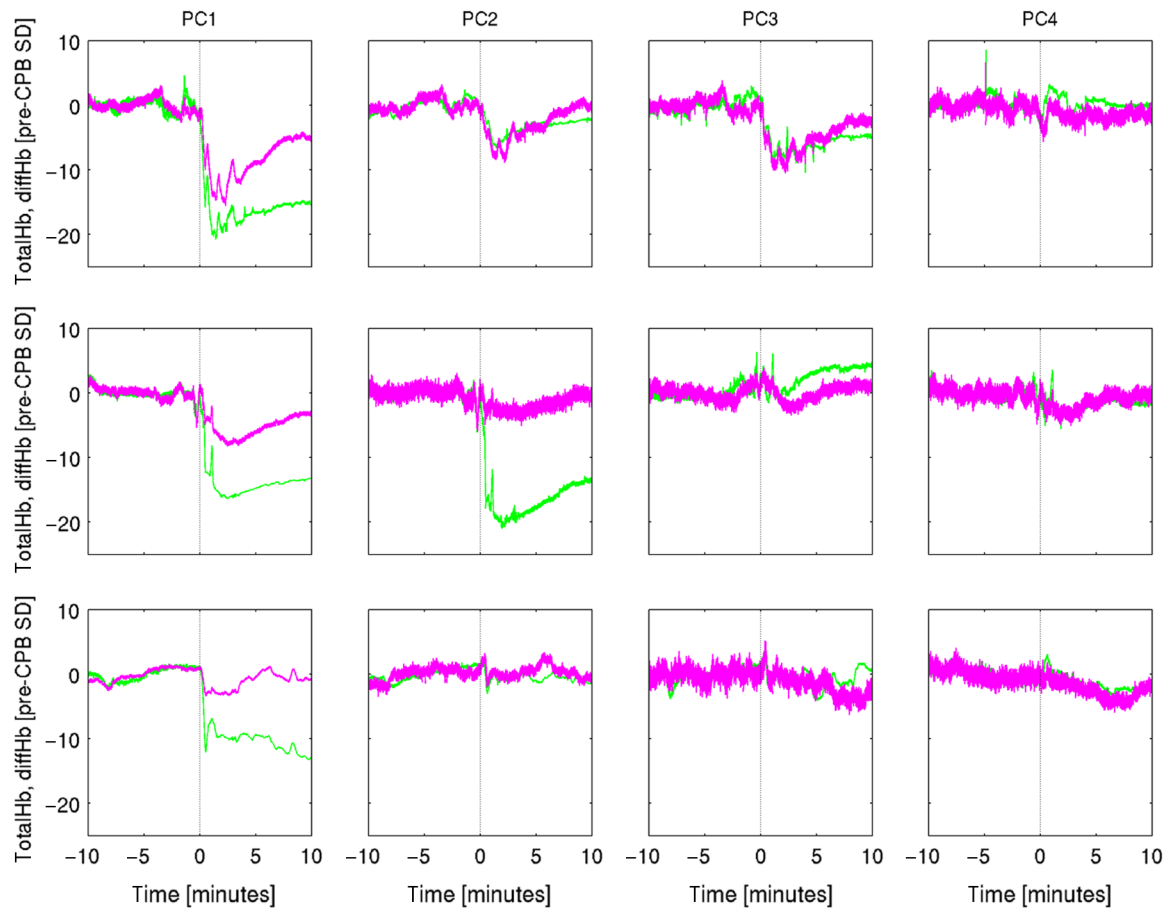


Fig. 5 Temporal evolution of totalHb and diffHb for the first four PCs. Displayed are epochs of 10 min prior and after CPB start at time zero (dotted vertical lines). Signals were normalized to zero mean and unit variance in the pre-CPB phase.

not shown). In patient #1, a decrease of totalHb and diffHb after CPB start was visible also in PC2 and PC3 and in patient #2 a drop of totalHb was visible in PC2. All other PCs were rather unaffected.

In contrast to the “global” components PC1, we found no PC that was categorized as “local” by our collectivity criteria as shown in Fig. 3.

PCs that were under-represented in left or right-frontal NIRS were more frequent. In patients #1 and #2, the vast majority of these PCs were also identified as artifact dominated based on visual inspection (46 out of 48, see Table 2). Exceptions were PC3 and PC4 of patient #2 (see Fig. 9 of the Appendix and Fig. 6 of the main text), which were underrepresented in right-frontal NIRS channels 56 to 59 and accounted for variance fractions of 0.0155 and 0.0119, respectively (roughly explaining 10% of amplitude variation each). They were localized in the left temporal (PC3) and the left-frontal region (PC4) and had no clear association with expected intraoperative oxygenation changes. The left-frontal NIRS channels 47 to 50 were sensitive to these events.

In contrast, only 11 and 13 of the 17 PCs that were under-represented in frontal left and right NIRS channels of patient #3 were clearly identified as artifact dominated. From the non-artifactual PCs, PC4 accounted for the largest normalized variance fraction of 0.0079 (i.e., ~9% of the total signal amplitude variations). The map shown in Fig. 6 reveals that this event was localized in NIRS channels recording from the perfusion

territories of the right MCA and consisted in a deviation of the right temporal versus all other channels.

In Fig. 7, we focus on the HCA phase of patient 3 and illustrate the temporal evolution of totalHb and diffHb for PC1 to PC4 as well as for exemplary original time series.

Table 2 Underrepresented PCs in left and right-frontal NIRS channels.

Patient	#1	#2	#3
Total number of PCs under-represented in left-frontal NIRS	13	12	17
Total normalized variance in these PCs	0.0117	0.0027	0.0144
PCs under-represented in left-frontal NIRS that were not identified as clear artifacts	0	0	6
Total number of PCs under-represented in right-frontal NIRS	17	6	17
Total normalized variance in these PCs	0.0421	0.0286	0.0198
PCs under-represented in right-frontal NIRS that were not identified as clear artifacts	0	2	4

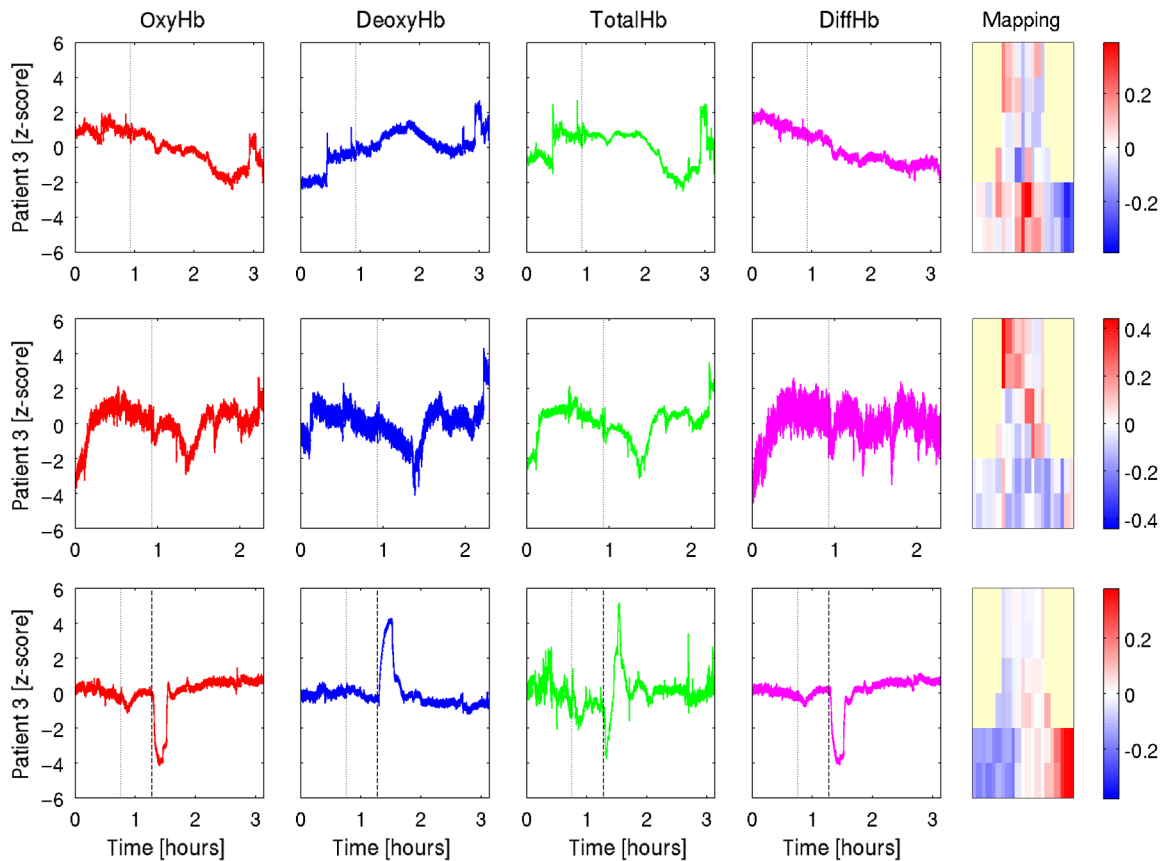


Fig. 6 Same as Fig. 4 but for PC4.

The intraoperative evolution of PC4 and the NIRS signal measured from the right temporal region (channel 31) reveal a steep and continuous decrease of diffHb during SACP. In contrast, left frontal (channel 47) and temporal NIRS signals (channel 1) showed the expected normalization of diffHb after SACP start, whereas right-frontal NIRS (channel 59) recorded constant diffHb during the full SACP phase. According to the map shown in Fig. 6, the trace of PC4 indicated hypoperfusion of the temporooccipital area, representing the dorsal MCA vascular territory and the MCA/PCA (posterior cerebral artery) watershed area. Clinically, this event resulted in a delayed return of miosis of the ipsilateral pupil during rewarming. As expected, pupils were maximally wide and unresponsive during HCA. This transient anisocoria had resolved by the end of surgery. Postoperatively, right after emergence the patient presented with transient nonspecific neurological signs of bilateral asterix, as well as an attention and orientation deficit. Furthermore, he developed a postoperative delirium with visual hallucinations.

4 Discussion

We report our findings of a pilot study of patients monitored with a spatially extended multichannel CW-NIRS device. During on-pump cardiac surgery multichannel recordings and data analysis proved largely artifact-free, and hence made brain oximetry mapping technically feasible in three patients.

One major regional desaturation episode was detected in patient #3 undergoing aortic arch surgery with HCA and SACP, which was followed by a clinical adverse event suggesting

a possible causal relationship. This incident would have been missed by a conventional intraoperative NIRS assembly that is restricted to bifrontal channels, emphasizing the relevance of our multichannel diagnostic tool. Bifrontal NIRS recording indicated sustained low or even recovering cortical oxygenation during SACP, whereas multichannel NIRS revealed progressive desaturation in recordings from the right temporal lobe despite ipsilateral SACP (Fig. 7).

Some possible explanations for the regional desaturation are right hemispheric and vertebra-basilar hypoperfusion due to SACP cannula malpositioning in the brachiocephalic trunk (e.g., toward the right subclavian artery), or runoff of right-sided SACP flow or partial outflow obstruction of the right SACP cannula.^{29,30} An alternative explanation might be particulate or air embolism to the right MCA, affecting oxygen supply to only parts of its vascular territory.^{31,32} At any rate, oxygen delivery by the SACP to the right ACA appeared slightly less than to the left ACA area but sufficient to prevent progressive right-frontal tissue oxygen desaturation. This indicates that the right ACA territory received its blood via the anterior communicating artery of the CoW from SACP to the left common carotid artery (CCA).¹⁹ Both the right vertebral artery (VA) and the right ICA are supplied by the brachiocephalic trunk. The transient anisocoria during the operation can be explained by hypoperfusion of the vertebrobasilar system, especially the right PICA, which is a branch of the right VA. Restricted blood flow of the right ICA and MCA with subsequent hypoperfusion of the temporal lobe as confirmed by NIRS may be the cause of the postoperative complex neurological deficits in attention and orientation.^{33,34} Apparently, the

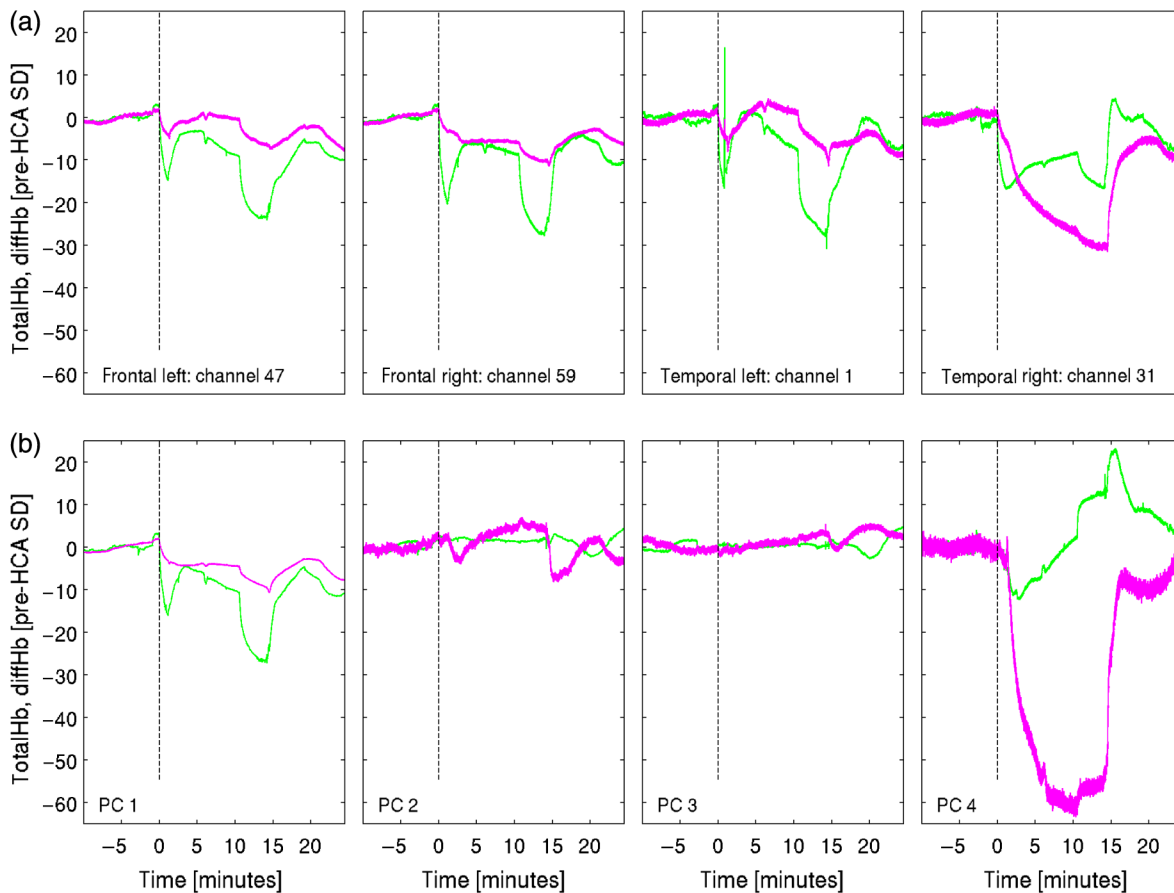


Fig. 7 Malperfusion of the right MCA in patient #3 during HCA with SACP. Shown is totalHb and diffHb in an epoch of 10 min prior and 25 min after HCA start at time zero (dashed vertical lines). The HCA period lasted for 14 min and SACP lasted from minute 1 to 11. All signals were normalized to zero mean and unit variance in the pre-HCA phase. (a) Four representative NIRS channels and (b) nonartifactual localized PC1 to PC4.

blood flow to the left cerebral hemisphere—supplied through SACP of the left CCA—remained stable during HCA (Fig. 7).

This observation reinforces concerns of clinicians that commercially available bilateral frontal NIRS oximetry lacks the sensitivity to detect malperfusion of the temporal or parietal brain regions. SACP is a standard technique in aortic arch surgery to maintain cerebral perfusion and cooling during HCA, to avoid the cerebral metabolic deficit observed after HCA without SACP. Risks of the technique are introduction of emboli into the cerebral circulation, cannula misplacement, vessel dissection, and malperfusion; conversely, high perfusion pressures with cerebral hypercirculation have the potential to provoke cerebral edema.^{35,36}

The main limitation of this pilot study is the small number of participants. Assuming a mean incidence of 1% for severe intraoperative neurological adverse events,² one would need to enroll 161 patients to observe at least one such event with a probability of >80% (binomial model). Also, the advantage of extended spatial coverage of MCA and ACA territories with this type of multichannel CW-NIRS device (Fig. 1) is somewhat reduced by its limitation of measuring relative hemoglobin concentration changes rather than absolute oxyhemoglobin concentrations and fractional saturation.

Another limitation yet to be overcome in multichannel NIRS, recordings with currently available commercial systems are

movement artifacts. Recordings from one initial test patient contained many artifacts from OR table movements with volatility dominating the whole recording and not limited to a few components after PCA. In contrast, the three following patients had only few such artifacts and thus qualified for quantitative analysis. Nonetheless, the data had to be carefully inspected to prevent misinterpretation of minor movement artifacts as physiological changes. During two of the analyzed cases, all major physiological variations in the NIRS signal were detectable by at least one of the conventional measurement positions on the left or right forehead. In technical terms, this means that after exclusion of clearly artifact dominated PCs and after FDR correction for multiple comparisons, none of the remaining PCs were statistically under-represented at both frontal NIRS locations at the same time. In clinical terms, the frontal NIRS channels represent frontal and temporoparietal territories only when there is no perfusion deficit of the temporoparietal region. Artifact control is only one of the reasons why the technique of multichannel NIRS is time consuming to set up and not yet feasible for routine use during cardiac surgery.³⁷ The development of a clinically feasible device for monitoring oxygen saturation in the ACA and MCA regions might prove useful to further reduce the incidence of severe adverse neurological events during high risk cardiac surgical interventions and especially during thoracic aortic surgery.

Typically, a stroke of the MCA region presents with contralateral brachiofacial hemiparesis and perceptual deficits, such as hemispatial neglect, anosognosia, apraxia, and spatial disorganization in case of a nondominant hemispheric lesion.³⁴ Our patient #3 did not exhibit those signs, which might be explained by hypothermic brain protection, a reduction but not complete cessation of blood flow to the MCA territory, and full recovery of flow after HCA. Furthermore, HCA time was 14 min, which included 10 min of SACP. The desaturation event shown in Fig. 7 lasted exactly for the duration of HCA. Despite communication of a presumed right cannula malpositioning to the surgeon, his attempt to adjust it did not restore hemoglobin levels over the affected MCA region to normal. An embolic event or another faulty redirection toward the subclavian artery may have occurred, since successful correction of the cannula position is reported to result in an immediate improvement of regional cerebral oxygenation. A recent publication of a case with SACP—which was complicated by a right-sided frontal NIRS reduction—demonstrated that repositioning of the cannula can restore oxygenation within seconds.²⁹ Another trial in patients undergoing coronary artery bypass graft surgery, which assessed the frequency of frontal cerebral oxygen desaturation during CPB and the efficacy of an intervention algorithm to redress it recorded failure to restore oxygenation in only 5%

of desaturation events. However, possible reasons for failure to restore oxygenation in these cases and its consequences were not further discussed.¹²

In conclusion, in this pilot study we found that spatially extended NIRS monitoring with coverage of both frontal and temporal regions might improve the detection and localization of critical tissue hemoglobin desaturation events of both cerebral hemispheres. More research on multichannel NIRS monitoring during cardiovascular surgery is necessary and should focus on scenarios of thoracic aortic procedures with well-defined cerebral perfusion strategies and neurological event rates to possibly reduce consequences of ischemia and improve post-operative outcome.

Appendix

Full intraoperative recordings of PC2 and PC3 are displayed in Figs. 8 and 9, respectively. Figure arrangement is identical to Fig. 4: CPB start is indicated by dotted vertical lines and HCA start in patient 3 by dashed vertical lines. PC2 explains between 3% and 10% and PC3 between 1% and 3% of the total variance. In contrast to PC1 (Fig. 4), the collectivity of these components varies in the normal range between 0.18 and 0.39 (see Fig. 3).

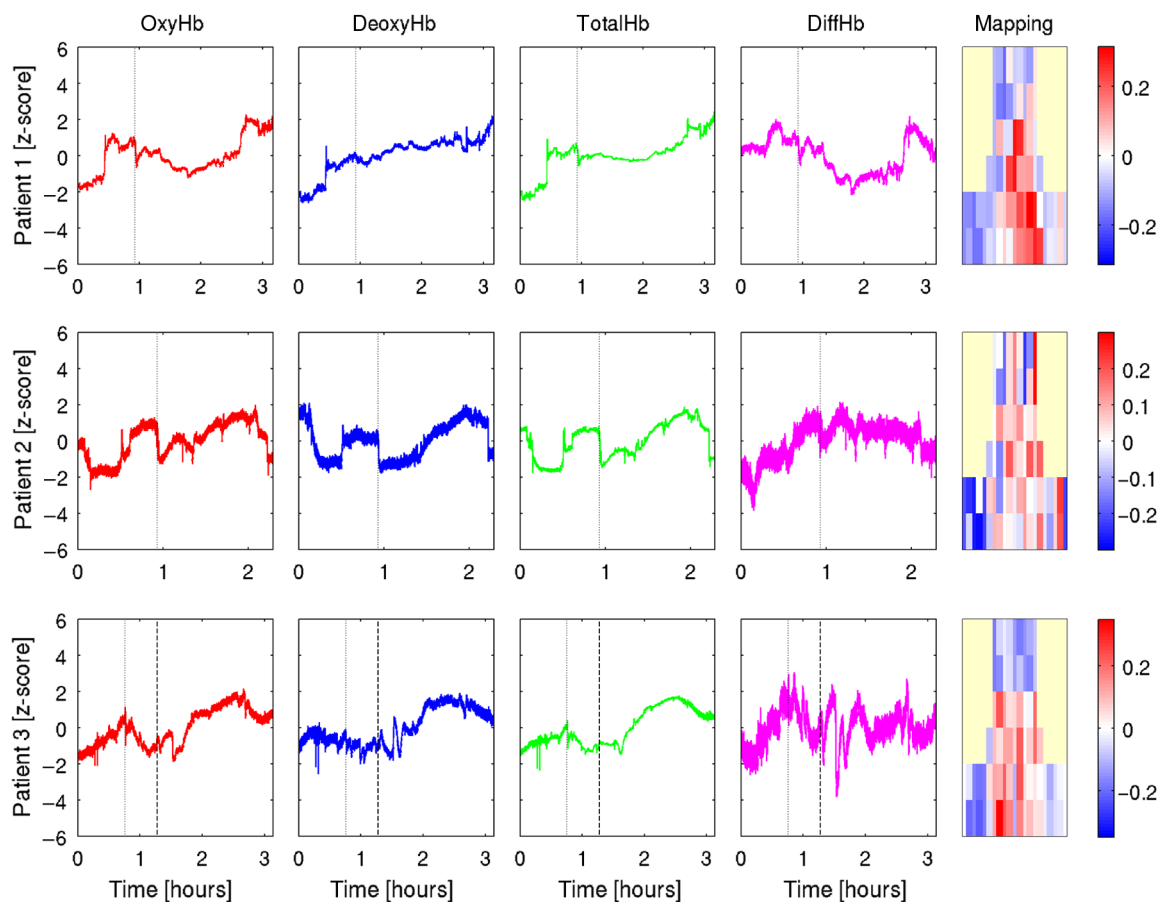


Fig. 8 Displayed are the full intraoperative recordings for PC2. CPB start is indicated by dotted vertical lines and HCA start in patient 3 by dashed vertical lines. For spatial orientation of the maps and interpretation of the patches, refer to the right part of Fig. 1. No signals were recorded in the yellow shaded areas.

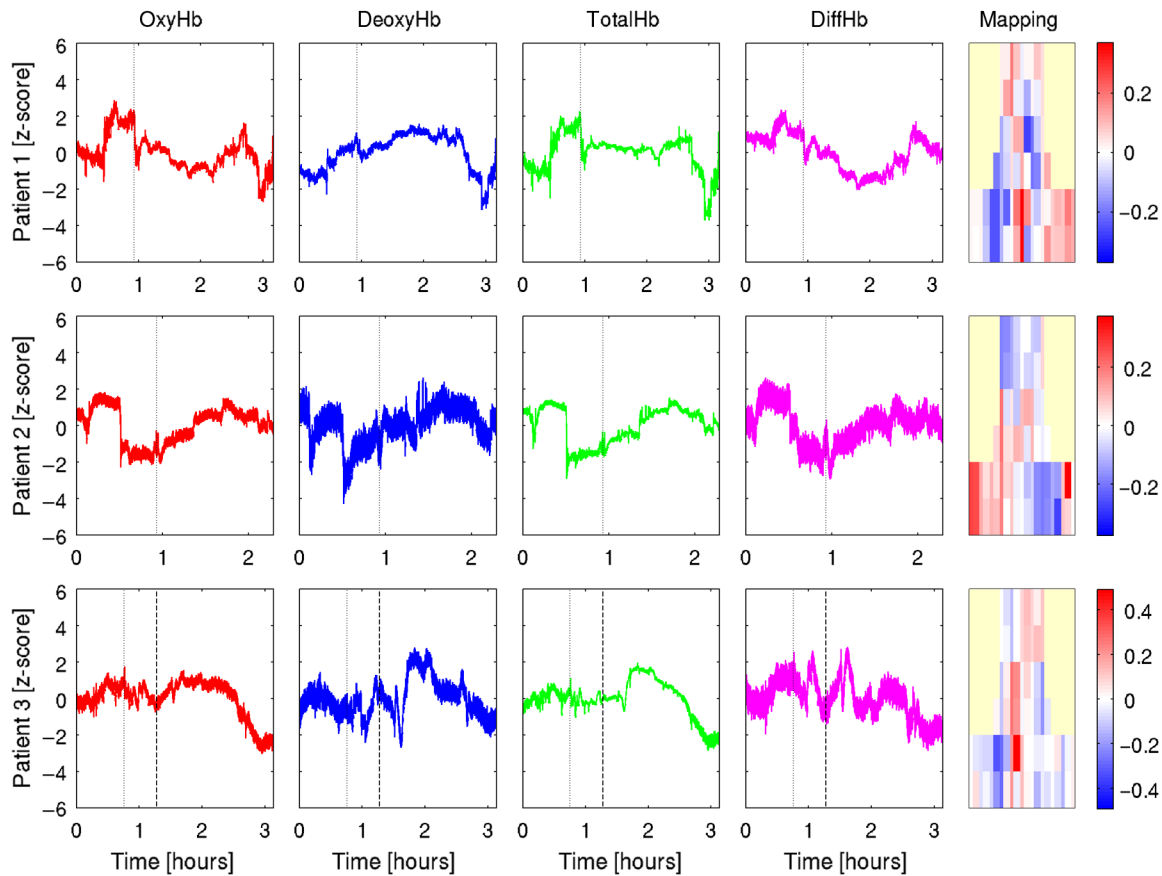


Fig. 9 Displayed are the full intraoperative recordings for PC3. CPB start is indicated by dotted vertical lines and HCA start in patient 3 by dashed vertical lines. For spatial orientation of the maps and interpretation of the patches, refer to the right part of Fig. 1. No signals were recorded in the yellow shaded areas.

Disclosures

No conflicts of interest, financial or otherwise, are declared by the authors.

Acknowledgments

The authors thank PhD Darren Hight for proofreading the final article.

References

- J. Bucnerius et al., "Stroke after cardiac surgery: a risk factor analysis of 16, 184 consecutive adult patients," *Ann. Thorac. Surg.* **75**(2), 472–478 (2003).
- G. M. McKhann et al., "Stroke and encephalopathy after cardiac surgery: an update," *Stroke* **37**(2), 562–571 (2006).
- L. Harvey et al., "Stroke after left ventricular assist device implantation: outcomes in the continuous-flow era," *Ann. Thorac. Surg.* **100**(2), 535–541 (2015).
- C. W. Hogue et al., "Risk factors for early or delayed stroke after cardiac surgery," *Circulation* **100**(6), 642–647 (1999).
- D. S. Likosky et al., "Determination of etiologic mechanisms of strokes secondary to coronary artery bypass graft surgery," *Stroke* **34**(12), 2830–2834 (2003).
- D. A. Scott, L. A. Evered, and B. S. Silbert, "Cardiac surgery, the brain, and inflammation," *J. Extra Corpor. Technol.* **46**(1), 15–22 (2014).
- F. Zheng et al., "Cerebral near-infrared spectroscopy monitoring and neurologic outcomes in adult cardiac surgery patients: a systematic review," *Anesth. Analg.* **116**(3), 663–676 (2013).
- J. Stepan and C. W. Hogue, "Cerebral and tissue oximetry," *Best Pract. Res. Clin. Anaesthesiol.* **28**(4), 429–439 (2014).
- G. Vretzakis et al., "Cerebral oximetry in cardiac anesthesia," *J. Thorac. Dis.* **6**(Suppl. 1), S60–S69 (2014).
- K. M. Brady et al., "Noninvasive autoregulation monitoring with and without intracranial pressure in the naive piglet brain," *Anesth. Analg.* **111**(1), 191–195 (2010).
- P. E. Bickler, J. R. Feiner, and M. D. Rollins, "Factors affecting the performance of 5 cerebral oximeters during hypoxia in healthy volunteers," *Anesth. Analg.* **117**(4), 813–823 (2013).
- B. Subramanian et al., "A multicenter pilot study assessing regional cerebral oxygen desaturation frequency during cardiopulmonary bypass and responsiveness to an intervention algorithm," *Anesth. Analg.* **122**(6), 1786–1793 (2016).
- D. Hori et al., "Arterial pressure above the upper cerebral autoregulation limit during cardiopulmonary bypass is associated with postoperative delirium," *Br. J. Anaesth.* **113**(6), 1009–1017 (2014).
- B. Joshi et al., "Predicting the limits of cerebral autoregulation during cardiopulmonary bypass," *Anesth. Analg.* **114**(3), 503–510 (2012).
- A. Galimani et al., "Endovascular therapy of 623 patients with anterior circulation stroke," *Stroke* **43**(4), 1052–1057 (2012).
- M. R. Heldner et al., "National Institutes of Health stroke scale score and vessel occlusion in 2152 patients with acute ischemic stroke," *Stroke* **44**(4), 1153–1157 (2013).
- S. A. Gunnal, M. S. Farooqui, and R. N. Wabale, "Anatomical variations of the circle of Willis in cadaveric human brains," *Neurol. Res. Int.* **2014**(1), 687281 (2014).
- S. R. Naveen, V. Bhat, and G. A. Karthik, "Magnetic resonance angiographic evaluation of circle of Willis: a morphologic study in a tertiary hospital set up," *Ann. Indian Acad. Neurol.* **18**(4), 391–397 (2015).

19. J. Hendrikse et al., "Relation between cerebral perfusion territories and location of cerebral infarcts," *Stroke* **40**(5), 1617–1622 (2009).
20. C. Rummel et al., "Monitoring cerebral oxygenation during balloon occlusion with multichannel NIRS," *J. Cereb. Blood Flow Metab.* **34**(2), 347–356 (2013).
21. A. Devor et al., "Frontiers in optical imaging of cerebral blood flow and metabolism," *J. Cereb. Blood Flow Metab.* **32**(7), 1259–1276 (2012).
22. J. P. Vandenbroucke et al., "Strengthening the reporting of observational studies in epidemiology (STROBE): explanation and elaboration," *PLoS Med.* **4**(10), e297 (2007).
23. D. T. Delpy et al., "Estimation of optical pathlength through tissue from direct time of flight measurement," *Phys. Med. Biol.* **33**(12), 1433–1442 (1988).
24. F. Scholkmann et al., "A review on continuous wave functional near-infrared spectroscopy and imaging instrumentation and methodology," *NeuroImage* **85**(1), 6–27 (2014).
25. I. T. Jolliffe, "Principal component analysis and factor analysis," in *Principal Component Analysis*, Springer, New York (2002).
26. M. Müller et al., "Detection and characterization of changes of the correlation structure in multivariate time series," *Phys. Rev. E* **71**(4), 046116 (2005).
27. C. Rummel et al., "A systems-level approach to human epileptic seizures," *Neuroinformatics* **11**(2), 159–173 (2013).
28. C. R. Genovese, N. A. Lazar, and T. Nichols, "Thresholding of statistical maps in functional neuroimaging using the false discovery rate," *NeuroImage* **15**(4), 870–878 (2002).
29. S. K. C. Chan et al., "Cannula malposition during antegrade cerebral perfusion for aortic surgery: role of cerebral oximetry," *Can. J. Anesth.* **61**(8), 736–740 (2014).
30. K. Orihashi et al., "Malposition of selective cerebral perfusion catheter is not a rare event," *Eur. J. Cardio-Thorac. Surg.* **27**(4), 644–648 (2005).
31. G. B. Mackensen et al., "Cerebral embolization during cardiac surgery: impact of aortic atheroma burden," *Br. J. Anaesth.* **91**(5), 656–661 (2003).
32. C. W. Hogue, R. F. Gottesman, and J. Stearns, "Mechanisms of cerebral injury from cardiac surgery," *Crit. Care Clin.* **24**(1), 83–98 (2008).
33. A. Nouh, J. Remke, and S. Ruland, "Ischemic posterior circulation stroke: a review of anatomy, clinical presentations, diagnosis, and current management," *Front. Neurol.* **5**, 30 (2014).
34. J. S. Kim and L. R. Caplan, "Clinical stroke syndromes," *Front. Neurol. Neurosci.* **40**, 72–92 (2016).
35. D. K. Harrington, F. Fragomeni, and R. S. Bonser, "Cerebral perfusion," *Ann. Thorac. Surg.* **83**(2), S799–S804 (2007).
36. N. Khaladj et al., "Hypothermic circulatory arrest with selective antegrade cerebral perfusion in ascending aortic and aortic arch surgery: a risk factor analysis for adverse outcome in 501 patients," *J. Thorac. Cardiovasc. Surg.* **135**(4), 908–914 (2008).
37. Y. Shingu et al., "Real-time cerebral monitoring using multichannel near-infrared spectroscopy in total arch replacement," *Jpn. J. Thorac. Cardiovasc. Surg.* **51**(4), 154–157 (2003).

Christian Rummel received his PhD in theoretical nuclear physics in 2004. Thereafter, he changed to time series analysis and started to investigate multivariate neurophysiological signals (EEG and fMRI of epilepsy patients and NIRS recordings). Since 2010, he has been working in neuroradiology, mainly evaluating structural MRI of patients and healthy controls morphometrically.

David Reineke studied medicine at the Albert-Ludwigs-University in Freiburg, Germany, and graduated in 2004. He started his formation as a cardiac surgeon in Basel, Switzerland, and later changed to the University Hospital Bern, Switzerland, where he became consultant in 2011 and senior consultant under Professor Thierry Carrel in 2016. His main interest lies in heart failure surgery. Together with Professor Lars Englberger, he is responsible for VADs and transplants in their unit.

Balthasar Eberle is a senior consultant in cardiovascular anaesthesia and associate professor at the University Hospital Bern. He was a director in the Cardiothoracic Anesthesia Division, Johannes Gutenberg University Medical School, Mainz, Germany, until 2003. He was an attending anesthesiologist and research fellow at Johns Hopkins University School of Medicine, Baltimore, Maryland, USA, from 1989 to 1991. He received his diploma degree from the Management of Healthcare Institutions, University of Kaiserslautern, Germany. His received board certifications in anesthesiology in 1987 with subspecialties intensive care and emergency medicine and his medical diploma and doctorate at Ludwig Maximilians University and Institute of Surgical Research, Munich, Germany, in 1982.

Heiko A. Kaiser graduating from medical school in 2002 in Heidelberg, Germany, training in anesthesia at the university hospital in Bern, Switzerland, and completing a cardiac anesthesia fellowship thereafter. He is a research fellow from 2004 to 2005 and a visiting professor from 2010 to 2013 at Washington University in St. Louis, Missouri, USA, where he got interested in brain monitoring during (cardiac) anesthesia and involved in outcome studies. He has been an attending physician in cardiac anesthesia in Bern, Switzerland, since 2009. His recent projects are on cerebral autoregulation, NIRS, and epileptic potentials during cardiac surgery.

Biographies for the other authors are not available.